-RESEARCH PAPER

International Journal of Mining and Geo-Engineering

IJMGE

IJMGE 59-4 (2025) 333-340

DOI: 10.22059/IJMGE.2025.395411.595251

A coupled empirical-numerical method for open-stope stability analysis considering stope dimensions

Hassan Mohammadi [a], Mohammad Fatehi Marji [a, *], Seyed Mohammad Esmaeil Jalali [b] and Ali Dabbagh [a]

[a] *Department of Mining and Metallurgical Engineering, Yazd University, Yazd, Iran.*

[a] *Faculty of Mining Engineering., Petroleum and Geophysics, Shahrood University of Technology, Shahrood, Iran,*

Article History:

Received: 16 May 2025.

Revised: 16 July 2025.

Accepted: 27 August 2025.

ABSTRACT

Most of the empirical methods are used for analyzing the stability of open stopes in underground mining and share common features based on two main factors: the interplay between geomechanical (mechanical characteristics) and geometrical (shapes and dimensions) parameters of the rock and orebody. The width of stopes is somewhat controllable, given the consistent strength and mechanical properties of the ore and its country rock. The dimensions of stable stopes are estimated using the "hydraulic radius" and "radius factor", which are the primary geometric factors after considering uncontrollable factors, such as the mechanical behavior of the ore and its country rock, environmental measures, safety, and the overall height of the orebody. Essentially, the influence of the stope's geometry, particularly its width, is equivalent to that of all other uncontrollable factors for a specific ore deposit. The hydraulic radius is inherently two-dimensional, leading to the consideration of only the length and height of the stope in its safe design. However, this approach overlooks the smallest dimension (third dimension), typically the thickness of the ore vein, despite evidence from observations and empirical studies indicating that all three dimensions of mining stopes can influence their stability during the ore extraction period. To address the neglecting of the third dimension in evaluating open stope stability, this article presents numerical models of various stopes with similar geomechanical characteristics but differing dimensions, analyzed using an explicit finite difference approach. The results are then assessed to understand how the third dimension impacts the hydraulic radius and, consequently, the stability conditions of the open stopes. Ultimately, a new mean modified hydraulic radius (MHR) is introduced to assess the influence of the ore body thickness on the stability analysis of open stope mines.

Keywords: *Open stopes; Numerical & empirical methods; Stope width; Stability analysis; Hydraulic radius..*

1. Introduction

Underground open stope mining typically creates large open spaces, a defining feature of this method. Consequently, instability in these areas after ore extraction can lead to severe consequences and disasters. Thus, prioritizing sustainability during the mine design phase and selecting a reliable mining method are crucial technical considerations in modern mining practices.

Both natural factors (related to the stope construction environment) and manmade factors (such as operational considerations and stope geometry) influence the stability of mining stopes and underground spaces. Meanwhile, when analyzing mine stability conditions, only the values of unnatural factors, especially the geometry of the stope, can be controlled and are at the disposal of the designer. The existing empirical methods of mine stability analysis show that the effects of stope geometry have been specially considered in almost all the methods. In most of the analyses, the hydraulic radius or radius factor can be seen on one axis and other effective factors such as geomechanical characteristics, environmental factors, etc. can be seen on the other axis which indicates the significant role and importance of stope geometry in the design of underground mining methods. In the existing empirical equations for the stability analysis of open stopes, the hydraulic radius index and the radius factor, which represent only some of the geometric characteristics of the stope, are considered. The hydraulic radius is a two-parameter factor with a two-dimensional concept, and is obtained by dividing the stope area by the perimeter in a section parallel to the hanging wall (and footwall) of the ore deposit, and it only expresses the effect of two dimensions of the stope on its stability. Open stopes with a high slope, such as the sublevel stope shown in Figure 1-a, in addition to the length and height that express the surface of the stope, also have a smaller dimension that can be called the third dimension or the width of the stope. Indeed, it refers to the thickness of the ore vein. Despite the existence of objective experiences and engineering evidence that all dimensions of the stope have an impact on its stability, in the present empirical methods of stability analysis, the impact of the third dimension has been ignored (which is considered a deficiency of the empirical methods). As a result, the hydraulic radius alone cannot be a good representative of the geometry of the stope, so in order to obtain a more complete and appropriate empirical approach, it is necessary to modify the method of estimating the hydraulic radius or to extract a more comprehensive geometric index or indices in addition to the hydraulic radius, which includes a greater number of the geometric features of the extraction stope. On the other hand, there are some open stopes with a low slope angle, such as the room and pillar stopes shown in Figure 1-b. In these types of stopes, the third dimension is equivalent to the height of the stope. This research was done with the aim of

* Corresponding author. *E-mail address:* mohammad.fatehi@gmail.com (M. Fatehi Marji).

improving the role of stope geometry on its stability and evaluating the impact of the third dimension on the stability of open stopes mines.

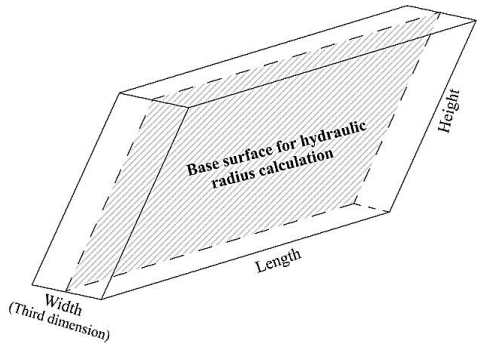

a: Open stope with a high slope, such as the sublevel stope method.

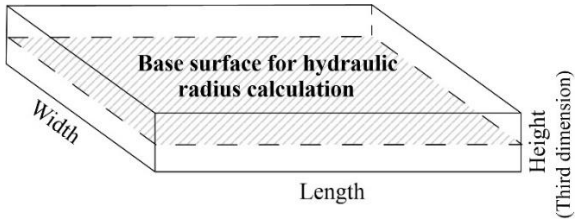

b: Open stope with a low slope, such as the room and pillar stope method

Figure 1. Demonstration of the third dimension of the stope in open stopes mining methods (with a low slope and with a high slope).

2. Literature review and theoretical background on the stability of open stopes

The stability of open stopes has always been the focus of a large number of researchers. For this purpose, several methods, such as experimental, analytical, numerical, and empirical methods have been used for the design of open stope mines.

The empirical method of analyzing the stability of open stopes was first established in 1981 by Mathews, and extended by Mawdesley in 2001 [1,2]. Since then, a large number of researchers have collected new data from various mines with different depths and rock mass conditions, as a result of which Mathews's method was expanded and its effectiveness confirmed [3]. Mathews's original method is based on the analysis of more than 26 case studies from three Canadian underground mines and 29 cases of information retrieved from these sources, and includes the main factors influencing the design of open stopes [4]. In 2001, Mathews's stability graph was revised by Mawdesley, using data from over 400 mines. A few years later, based on the developed stability database, Mawdesley used logistic regression analysis to determine the boundary between stable and caving areas, the results of which are shown in Figure 2 [5].

As seen in Figure 2, the stability analysis is based on two parameters, stability number (N) and shape factor or hydraulic radius (HR). The stability number is located on the vertical axis and indicates the quality of the rock mass around the open stope. The stability number, N shows the ability of the rock mass to maintain stability under the existing stresses (geomechanical aspects), and the HR located on the horizontal axis is used to express the effect of stope geometry. Adjustment coefficients should be used to consider induced stresses and extraction direction. The estimation of aggregate quality is done using the Q ´ classification system. The value of Q ´ can be calculated from equation (1).

$$Q' = \frac{RQD}{J_n} \times \frac{J_r}{J_a} \quad (1)$$

In which:

RQD: Rock quality designation

J_n: Joint number related to the number of joint sets in the Q classification system

J_r: Joint roughness number in the Q classification system

J_a: Joint alteration number in the Q classification system

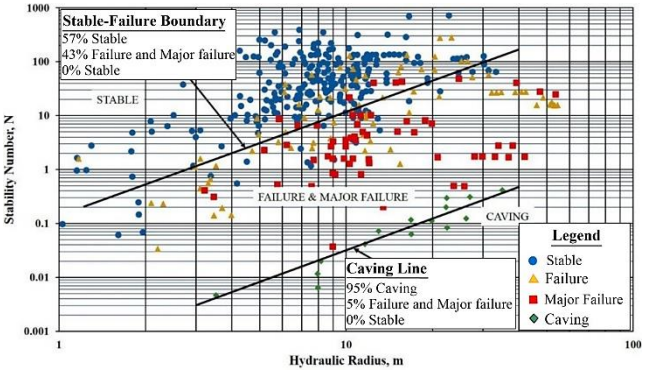

Figure 2. The modified Mathews's stability graph for open stope mines [5].

The stability number according to equation (2) is obtained from the product of Q´ and the adjustment coefficients for induced stresses, discontinuity direction, and working front direction.

$$N = Q' \times A \times B \times C \quad (2)$$

In which:

A: Rock stress factor

B: Joint orientation adjustment factor

C: Gravity adjustment factor

The diversity and multiplicity of research conducted on empirical methods of stability analysis since 1981 show that this issue has been the focus of researchers' attention and has been welcomed by many scholars in mining engineering. As an example, Mathews's method was modified and improved in the past years by Potvin [6,7-8], Nixon, and Hadjigeorgiou [9,10], Trueman [11], Stewart and Forsyth [12], Mawdesley and Trueman [13], Mawdesley [5], Suorineni [14], Mortazavi and Osserbay [3], and Suorineni and Madenova [15]. In the conducted research, both geomechanical characteristics and geometrical factors have been considered, but the focus has been more on geomechanical factors (i.e., improving the stability number). Nevertheless, considering the importance of stope geometry as a controllable factor affecting its stability, while focusing and paying attention to geomechanical factors, a number of researchers have evaluated and modified the impact of stope geometry on its stability. Table 1 shows the most important studies that have been done in this field.

While many research worked on the geometrical aspects of the stope using empirical methods in the past few decades, several issues remain unresolved. Milne et al. [16, 17] examined the stability of the stope's hanging wall and its geometry. In a subsequent study, Milne [18] addressed the shortcomings of the hydraulic radius in reflecting the stope's geometry and its effects on the stability analyses of open stope mining methods. To improve upon these deficiencies, he introduced a new index called the radius factor, which partially addressed some of the problems associated with the hydraulic radius. Some other researchers such as Germain et al. [20] also paid attention to the issue of stope geometry in the empirical methods of stability analysis and tried to improve the stope geometry by proposing a volumetric index. In some cases, especially, the lack of response in the dimensional ratio of the stope was noted. In a research, Henning and Mitri [22] highlighted the ineffectiveness of the hydraulic radius in some cases, especially the lack of response in the dimensional ratio of the stope. Basson [26] compared the hydraulic radius and the radius factor in his research and introduced

Table 1: History of research conducted on the effects of stope geometry on the stability analysis of open stope mining using the empirical methods.

Row	Researchers	Year	Subject
1	Milne et al.	1996	Quantification of hanging wall behavior
2	Milne et al.	1996	Estimation of surface geometry in open stopes
3	Milne	1997	Identifying the defects of the hydraulic radius and introducing the radius factor
4	Milne et al.	1997	Theory behind empirical design techniques
5	Germain & Hadjigeorgiou	1998	Suggestion of volumetric index
6	Milne et al.	2004	Interpreting hanging wall deformation in mines
7	Henning & Mitri	2006	Expressing the relationship between the hydraulic radius of the stope and the dimensional ratio
8	Andrews & Barsanti	2008	Results of the Radius Factor Stability Assessment Method for Design
9	Basson	2008	Comparing Hydraulic Radius (HR) and Effective Radius Factor (ERF)
10	Suorineni	2010	The stability graph after three decades in use
11	Milne et al.	2018	Prediction of hanging wall instability using the Strain Effective Radius Factor Method
12	Mohammadi et al.	2023	Analytical and comparative evaluation of empirical methods for stability studies of open stope with emphasis on the stope's geometry consideration

a software to calculate the radius factor. Also, Suorineni [14] stated the problems and shortcomings of stability diagrams and stated that one of the deficiencies of the empirical stability diagrams is due to oversimplification of the stope geometry. Mohammadi et al. [27] described and explained the limitations of using hydraulic radius (HR) and the radius factor (RF) for the analysis of open stopes. They presented a list of numerous shortcomings for assessing the effects of stope geometry on the stope stability when using HR and RF. One of the most important limitations of HR and RF is not considering the impact of the third dimension on the stability analysis of open stope mining.

3. Investigating the impacts of third dimension of open stopes in mine stability analysis

In most of the previous research, the effect of stope geometry on stability in empirical methods has been considered, generally with the hydraulic radius and to a limited extent with the radius factor. Additional research in this regard shows that these two indicators are able to approximately express the effects of stope geometry in the design of open stope mines. Also, the hydraulic radius index is effectively a two-dimensional factor and the impacts of the third dimension are ignored in the HR formulation. However, objective observations and empirical studies in open stopes show that the dimensions of mining stopes in all three dimensions can have an impact on their stability. The impact of the third dimension on instability (opposed to the stope stability conditions) has been proven as the effect of undercut height on undercuts driven in the stope mining methods [28]. The height of the undercut has an effect on various factors such as the induced stresses, the caving propagation paths and the flow of crushed ore, all of which have an effect on the rock instability. If the ability to destroy and crush the ore is high and the ore is broken easily, the undercutting height should be as low as possible (about one meter). This means that when the undercutting height is high, the possibility of the roof falling during the undercutting operation increases and the stability of the undercut decreases. On the other hand, if the ore has relatively good strength and its ability to be destroyed and crushed is low, the cutting height is increased to about 2 meters so that the conditions for optimal and suitable crushing can be provided in the ore deposit [29]. This issue shows that in addition to the surface of the undercut, the height (third dimension) of the excavated space under the cut is also effective in the failure of the roof of the excavated area. Since the subject of failure and stability of the stopes are complementary to one another, the effect of the third dimension of the extracted space on the stope stability analysis can be investigated accordingly.

To clarify the impact of the third dimension on stope stability, a conceptual example is presented. Figure 3 illustrates the simplified geometries of two open stopes, (a) and (b), both resembling sublevel stopes with steep slopes. While these stopes share equal geomechanical conditions, length, and height, stope (a) has a greater third dimension than stope (b). Scientific evidence, objective observations, and empirical studies demonstrate that, from a stability perspective, the behavior of these two stopes differs, despite their identical HR.

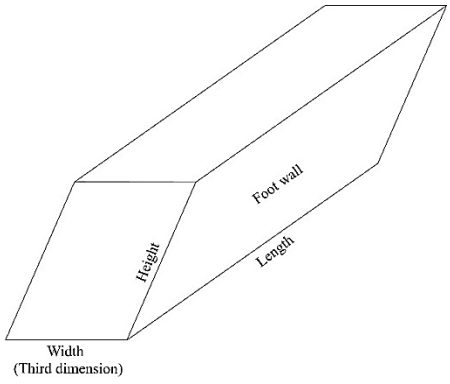

(a) The high slope stope with a thick width (third dimension is the ore vein thickness).

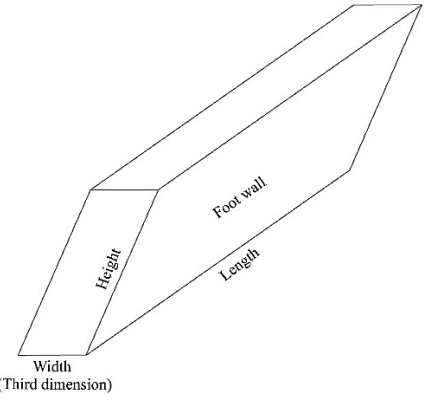

(b) The high slope stope with a thin width (third dimension is the thickness of the ore vein).

Figure 3: Comparison of the stability situations in high-slope stopes with different thicknesses (third dimensions).

Figure 4 also shows the simplified geometry of two open stopes with a low slope angle, similar to the room and pillar stopes. It is assumed that the mined stopes (a) and (b) have the same geomechanical conditions, and equal lengths and widths while the third dimension of stope (a) is greater than that of stope (b). The stability condition for stope (b) will not be similar to that of the stope (a).

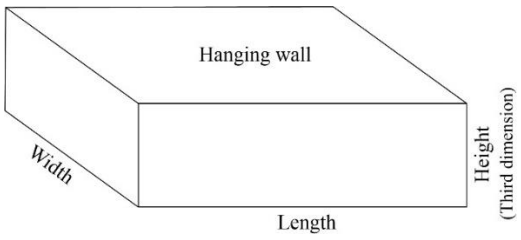

(a) The low slope stope with a thick width (third dimension is the vein height)

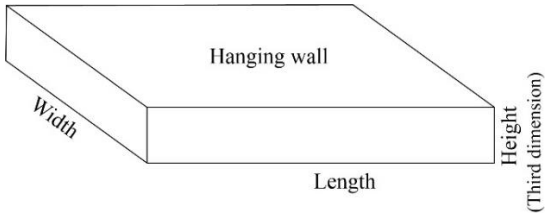

b) The low slope stope with a thin width (third dimension is the vein height)

Figure 4: Comparison of stability situations in open stopes with low slopes and different heights (third dimensions).

Figures 3 and 4 indicate that in open stopes, the third dimension is represented by the stope's width for vertical and high-slope stopes, while in horizontal (or low-slope) open stopes, it corresponds to the stope's height.

To analyze and compare the stability conditions of the stopes in Figures 3 and 4, an analytical study was conducted, focusing on the effect of the stope's third dimension on the stope's stability conditions based on elasticity theory. A cross-section of a horizontal stope (as shown in Figure 5) is modeled as a cantilever beam supported at both ends by the side pillars of the mining stope. The thickness of the ore, reflecting the height of the pillars on either side, varies, although the stope's width remains constant. The height of the pillar in stope (a) (Figure 4) is assumed to be greater than that of stope (b). This allows for the interpretation of the third dimension in horizontal stopes as analogous to a beam, aiding in the understanding of the research topic.

When an axial load F is applied to the roof of the stope, it affects a pillar with height L and cross-sectional area A, inducing stress σ and corresponding axial strain ε. Given that the pillar's modulus of elasticity is E and rigidity is K, we can derive the following relationships:

$$F = K.\Delta L \quad (3)$$

$$\sigma = \frac{F}{A} \quad (4)$$

$$\sigma = E.\varepsilon \quad (5)$$

$$\varepsilon = \frac{\Delta L}{L} \quad (6)$$

Considering the relationship between stress and strain in Equation (5) and the concept of stress and strain in Equations (4) and (6), Equations (7) and (8) can be obtained:

$$\frac{F}{A} = E.\frac{\Delta L}{L} \quad (7)$$

$$F = \frac{E.A}{L}\Delta L \quad (8)$$

Comparing equation (3) with Equation (8) results in Equation (9) as:

$$K = \frac{E.A}{L} \quad (9)$$

The stope pillar under axial force behaves similarly to a cylinder with rigidity K; increased axial rigidity enhances the pillar's resistance to deformation, making it harder.

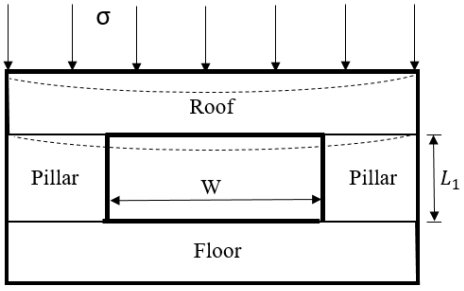

a: Stope with short pillars.

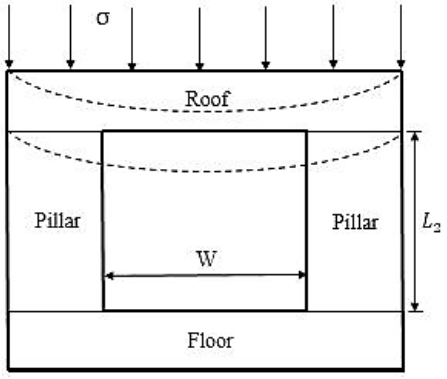

b: Stope with high pillars.

Figure 5: Comparison of the rigidity value of pillars for two horizontal stopes with different pillar heights.

With the pillar's cross-section, modulus of elasticity, and geomechanical conditions remaining constant, the rigidity of the pillar in stope (a) decreases due to the increased height, resulting in a larger denominator in the equation $K_2 = EA/L_2$. Consequently, the reduced rigidity (K_2) in stope (b) compared to stope (a) i.e., K_1 causes a shift in the roof's behavior from a double-headed beam supported close to stope conditions to one that experiences more strain, resembling articulated support conditions. Hence, as the pillar height increases in Figure (b) relative to Figure (a), the bending stress on the stope roof changes, impacting its stability. Therefore, it can be concluded that increasing the stope's height affects its stability through the pillar's height, a factor that must not be overlooked in the stability analysis of open stopes.

4. Numerical improvement of HR

The three-dimensional geometry of a stope, i.e., its length, width, and height, significantly influences its stability and serves as a crucial design parameter in underground open stope mining. Traditionally, empirical analyses of stope stability have focused primarily on the two larger dimensions, often overlooking the effects of the smaller dimension. To investigate the impact of this overlooked dimension, several open stopes with varying sizes but consistent conditions, such as depth, the horizontal-to-vertical stress ratio, and geomechanical characteristics of the ore and surrounding rocks were selected. These stopes were modeled using the finite difference method in FLAC^{3D} software. The stability of the walls for various stopes was evaluated, particularly emphasizing the smallest dimension while applying a uniform assessment criterion across all models. Table 2 displays the characteristics and assumptions of the modeled stopes.

Table 2: Specifications and assumptions for the main model of the open stope.

Row	Parameter	Symbol	Unit	Amount
1	Length	L	meter	1000
2	Height	H	meter	400
3	Model width	W	meter	400
4	Unit weight	ρ	tons per cubic meter	2.5
5	Depth	D	meter	250
6	The ratio of horizontal stress to vertical stress	K	-	1

Figure 6 shows that the load is applied vertically to the model. The model depth relative to the ground surface is 250 meters. To avoid an oversized model and computational complexity, 150 meters of this depth is modeled directly, while the remaining 100 meters of overburden is applied as surface loading to the top of the main model. The five lateral boundaries of the main block, in the directions perpendicular to the boundary faces, are fixed. This means that only the top face is allowed to displace.

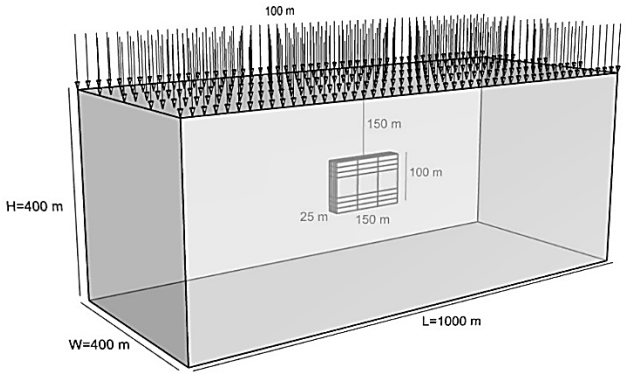

Figure 6: The dimensions, boundary conditions, and position of the stopes in the main numerical model.

This research models and analyzes three types of open stopes with wall stability assessed at widths (vein thickness) of 5, 15, and 25 meters. The specifications are as follows:

- Stope A: 50 meters long, 40 meters high
- Stope B: 100 meters long, 60 meters high
- Stope C: 150 meters long, 80 meters high

Table 3 displays the given input parameters used in the numerical modelling of the modeled stopes.

Table 3: FLAC3D input parameters based on the RocLab output parameters.

Row	Stope	Cohesion (MPa)	Phi (Degree)	Tension (MPa)	σ_{cm} (MPa)	E_m (GPa)
1	A5	0.46	31.3	0.0032	2.62	0.8
2	A15	0.48	31.9	0.0035	2.82	0.87
3	A25	0.5	32	0.004	3.03	0.94
4	B5	0.48	31.9	0.0035	2.82	0.87
5	B15	0.5	32.5	0.0038	3.03	0.9
6	B25	0.52	33.1	0.0042	3.24	0.97
7	C5	0.49	32.5	0.0038	3.03	0.9
8	C15	0.52	33.4	0.0044	3.35	0.99
9	C25	0.56	34.4	0.0053	3.69	1.12

Table 4 presents the dimensional specifications and classifications of these three open stopes. The hydraulic radius, calculated as the area divided by the perimeter (Equation (10)), is approximately 11 meters for class A stopes.

$$HR = \frac{A}{P} = \frac{2000}{180} = 11.11m \quad (10)$$

Table 4: Specifications and dimensions of the studied stopes A, B, and C.

Scenario	Symbol	Length (m)	Height (m)	Hydraulic radius (m)	Width (m)
1	A_5	50	40	11	5
	A_{15}				15
	A_{25}				25
2	B_5	100	60	18.75	5
	B_{15}				15
	B_{25}				25
3	C_5	150	80	26	5
	C_{15}				15
	C_{25}				25

Sakurai [30], based on field measurements, stated that if the strain level in the underground space does not exceed 1%, problems related to underground space instability will not occur. This statement was confirmed by Aydan et al. [31], Chern et al. [32], Hook [33], and Singh et al. [34]. The concept of critical strain is used as a threshold level for measuring increasing deformations.

In the stability assessment of open stope, the key consideration is that instability should not initiate during the extraction process. Therefore, in this research, the 1% strain threshold criterion proposed by Sakurai has been used.

The relative displacements of the stope walls along their smallest dimension are utilized to assess instability in mining stopes. In this study, a stope is considered unstable if the relative displacement of the wall exceeds a specified threshold, defined as one percent of the stope's height, measured in the third dimension (perpendicular to hanging wall). For instance, with a stope height of 40 meters, if the wall displacement exceeds 40 cm, the stope is considered unstable. This criterion is uniformly applied across all stopes.

In the first scenario, the stability of the stope wall is evaluated while assuming the fixed wall's surface, comparing stability across various widths (third dimensions). For example, in the first row (row 1) of Table 4, Class A stopes with a height of 40 meters and a length of 50 meters have a hydraulic radius of 11 meters, and the modelling examines widths of 5, 15, and 25 meters. The second scenario involves Class B stopes (row 2 of Table 4) with a hydraulic radius of 18.75 meters, also tested at widths of 5, 15, and 25 meters. The third scenario focuses on Class C stopes (row 3 of Table 4) with a hydraulic radius of 26 meters, modeled across the same widths.

The first scenario is analyzed by assuming that the instability in the stope wall occurs at a displacement exceeding 48 cm, which represents one percent of the stope's height. In the model, we assign various values for rock strength characteristics, such as the compressive strength of intact rock and the Geological Strength Index (GSI), while measuring the displacement in the stope wall. This process is iteratively refined until the stope wall displacement reaches 48 cm, allowing us to identify the rock mass characteristics corresponding to this value. In this case, the compressive strength of intact rock is 26 MPa, and the GSI is 18. Using these values along with Hooke's equations in ROCLAB software, the compressive strength of the rock mass in the hanging wall of the stope has been calculated as 2.62 MPa. The input parameters used in RocLab are listed in Table 5.

Figures 7, 8, and 9 illustrate the state of plasticity, displacement, and axial stress in the X-X direction, respectively, where the X-X direction corresponds to the stope's smallest dimension of 5 meters.

The plastic deformation process intensifies from the edge of the stope wall to the center, with a maximum displacement of 48 cm at the center, where the wall is stretched and the axial tensile stress reaches 900 Pa.

Table 5: RocLab input parameters.

Row	Stope	UCS (MPa)	GSI	m_i	D	Depth (m)	ρ (kg/m³)
1	A5	26	18				
2	A15	27	19				
3	A25	28	20				
4	B5	27	19				
5	B15	29	19	17	0	250	2500
6	B25	30	20				
7	C5	29	19				
8	C15	31	20				
9	C25	32	22				

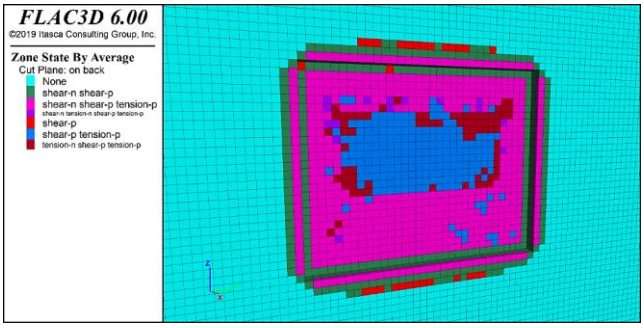

Figure 7: The state of plastic deformation in the stope with dimensions of 5, 40, and 50 meters.

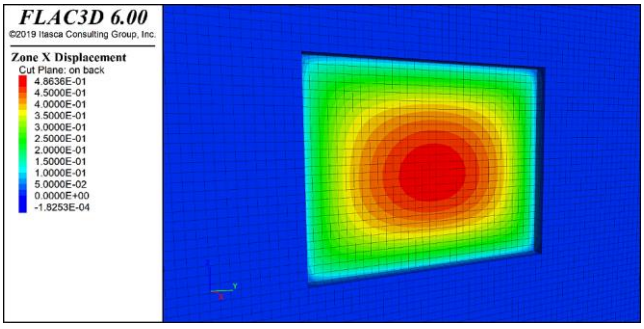

Figure 8: The state of the amount of displacement in the stope with dimensions of 5, 40, and 50 meters.

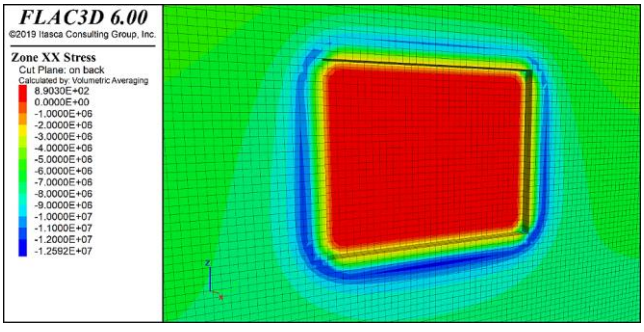

Figure 9: The state of axial stress along the third dimension in the stope with dimensions of 5, 40, and 50 meters.

Continuing with the first scenario, the dimensions and geometric shape of the stope wall remain unchanged (at a constant hydraulic radius). The strength characteristics corresponding to the 48 cm displacement are calculated for a stope width of 15 meters and another for 25 meters. For the stope of 15 meter in width, the compressive strength of the rock mass is 2.82 MPa, while for the 25-meter-wide stope, the compressive strength increases to 3.03 MPa.

For the second and third scenarios, modelling was conducted on Class B and C stopes listed in Table 3, with hydraulic radii of 18.75 meters and 26 meters, respectively. As in the first scenario, the compressive strength of the rock mass corresponding to displacements of 72 cm (1% of the wall height) and 96 cm was estimated for widths of 5 meters, 15 meters, and 25 meters. All results from the modelling of these scenarios are presented in Table 6.

Table 6 reveals that increasing the hydraulic radius, the dimensions of the wall surface and the negative impacts on stope stability. To maintain stability with an increased hydraulic radius, the rock's strength must be enhanced. For instance, in a stope with a hydraulic radius of 11 meters and a width of 5 meters, the wall rock's compressive strength is 2.62 MPa. If the hydraulic radius increases to 18.75 meters without changing the width, the compressive strength must rise to 2.82 MPa to ensure the stability of the stope walls.

Additionally, the data obtained from Table 6 also indicate that widening the stope reduces its stability conditions. In Class B stopes, for example, increasing the width from 15 meters to 25 meters necessitates raising the compressive strength of the wall rock from 3.03 MPa to 3.24 MPa to maintain the required stability of the stope. This pattern is similarly observed in Class A and Class B stopes presented in Table 6, highlighting the need to strengthen the wall rock as both hydraulic radius and width increase.

Further analysis of the data from Table 6, enables to compare the effects of hydraulic radius and stope width on stope stability. Increasing the stope width from 5 meters to 25 meters in class A increased the compressive strength of the stope wall rock mass from 2.62 MPa to 3.03 MPa.

This means that to maintain stability with a 20meter increase in width, the compressive strength of the rock mass needs to rise by 0.41 MPa. Additionally, if the hydraulic radius of a class A stope with a 5meter width (HR=11 meters) increases to 26 meters in a class C stope of the same width, the wall rock mass's compressive strength must also increase to maintain the stope stability. The similar changes in rock strength due to variations in hydraulic radius and stope width suggest that the impact of increased stope width (often deemed insignificant by some researchers) is indeed significant and should not be overlooked.

For a clearer understanding of the numerical analysis results from various scenarios in Table 6, see Figure 10.

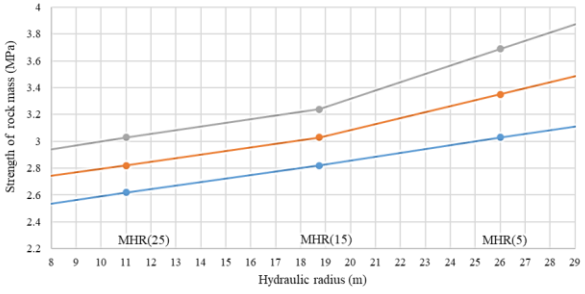

Figure 10 illustrates how stope stability varies with changes in hydraulic radius. The graph indicates that increasing the hydraulic radius (horizontal axis) necessitates a corresponding increase in the rock mass strength of the stope wall (vertical axis) to maintain stability. Furthermore, the modelling results for stopes of different widths allow for comparative analysis. The diagram shows that the intercept for the 5-meter-wide stope is lower than that of the 25-meter-wide stope, indicating that wider stopes have reduced stability and require increased rock mass strength for stability maintenance. Additionally, if a stope is stable at a specific hydraulic radius and width, widening the stope will necessitate achieving stability at a lower hydraulic radius. For instance, a stope stable at a hydraulic radius of 25 meters and a width of 5 meters would need to decrease the hydraulic radius to 17.5 meters for a width increase to 15 meters to maintain the same level of stability. If the stope width increases to 25 meters, the hydraulic radius must be reduced to approximately 10 meters in order to maintain stability. This assumes that the geomechanical characteristics of the rock mass remain unchanged with the change in thickness. This adjusted value represents

the modified hydraulic radius (MHR) for the new width. To explore the relationship between the MHR and the base hydraulic radius, an analysis of the data in Figure 10 has been conducted, leading to the formulation of Equation (11) for estimating the MHR.

$$(MHR)_C = (HR)_B \frac{2.24}{\sqrt{C}} \quad (11)$$

Where, $(HR)_B$ is the base hydraulic radius and can be calculated from Equation (12).

$$(HR)_B = \frac{a \times b}{2(a+b)} \quad (12)$$

and C is the width of the stope (thickness of the vein) or the third dimension and, $(MHR)_C$ is the Modified hydraulic radius for a stope with width C.

Regarding the applicable range of Equation 11, firstly, it is necessary to know that the minimum and maximum thickness of the ore vein for the implementation of open stope methods are typically between 5 and 30 meters [35]. Accordingly, the lower and upper bounds of the third dimension of the stope have been considered within this range.

Equation (11) was developed based on data extracted from the diagram shown in Figure 10. The third column in Table 7 presents the data extracted from this figure, which were used in the formulation of equation (11). In the fourth column of the same table, the values calculated using equation (11) are provided, and the representative correlation diagram is illustrated in Figure 11.

Table 7: Comparison of the results obtained from the diagram of Figure 10 and Equation (11).

Row	Thickness (m)	MHR (m) Obtained from Figure 10	MHR (m) calculated from equation (11)	Error (%)
1	15	8	8.91	10.2
2	25	8	10.21	21.6
3	5	9	9	0
4	15	9	9.7	7.2
5	25	9	10.66	15.5
6	5	10	10	0
7	15	10	10.29	2.8
8	25	10	11.2	10.7
9	5	11	11	0
10	15	11	9.71	13.2
11	25	11	11.65	5.5
12	5	12	12	0
13	15	12	11.51	4.2
14	25	12	11.87	1.1
15	5	13	13	0
16	15	13	12.03	8.1
17	25	13	12.1	7.4
18	5	14	14	0
19	15	14	12.55	11.5
20	25	14	12.9	8.5
21	5	15	15	0
22	25	15	16.42	8.6
23	5	16	16	0
24	25	16	16.88	5.2
25	5	17	17	0
26	25	17	17.4	2.3
27	5	18	18	0
28	25	18	17.97	0.2
29	5	19	19	0
30	25	19	18.54	2.5
31	5	20	20	0
32	25	20	19.59	2.1
33	5	21	21	0
34	25	21	20.6	1.9
35	5	22	22	0
36	25	22	21.6	1.8
37	5	23	23	0
38	25	23	22.69	1.3

As shown, a linear regression line has been fitted to the data, with a slope of 0.9454, which is very close to the ideal slope of 1, indicating a strong fit. The intercept of the fitted line is 0.8632, which is also within an acceptable range. Furthermore, the Coefficient of Determination (R^2) for the data fitted to the linear line is approximately 0.97, indicating a good linear relationship.

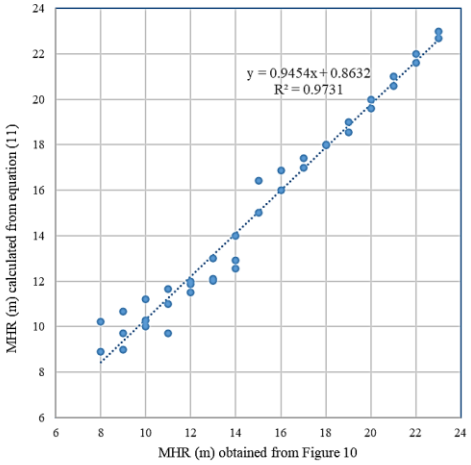

Figure 11: The correlation between the data obtained from Figure 10 and calculated from Equation (11).

5. Conclusion

In this research, the stability of underground open stopes is investigated based on the improvement of the existing empirical methods. In previous empirical methods, the geometry of the stope was typically represented by the Hydraulic Radius (HR) and limited by the Radius Factor (RF), which neglected the third dimension. Since the third dimension significantly impacts stope stability, ignoring it seems to be illogical. Therefore, this research introduces a new method that accounts for the third dimension in empirical stability analysis of open stope mines. The following main conclusions are gained:

- It is recommended to consider the stope width (C) in the stability graphs of open stopes in underground mining practice.
- The mean Modified Hydraulic Radius (MHR) can be used for considering the effects of the stope's third dimension on its stability conditions.
- The effects of stope width on the conventional HR can be obtained from the three-dimensional finite difference modelling of the open stope mining.
- The results of numerical modelling show that as the stope width increases the overall compressive strength of the surrounding rock mass increases to maintain the required stope stability conditions.
- New formulations are given for estimating the MHR based on the suggested numerical models considering the effects of the third dimension on the stability of open stopes.

Further development of the research may be conducted using the coupled analytical, numerical, and empirical methods for improving the evaluation of geometry effects on the overall open stope mine stability conditions.

References

[1] Mathews, K., Hoek, E., Wyllie, D., & Steward, S. (1981). Prediction of stable excavation spans for mining at depths below 1000 meters in hard rock mines. CANMET report DSS, Serial No. 0SQ80-00, Vol. 81.

[2] Mawdesley, C. A., Trueman, R., & Whiten, W. (2001). Extending the Mathews stability graph for open-stopee design, Trans.

Institut. Min. Metallurgy. (Section A: Mining Industry), 110, A27–A39. Doi: https://doi.org/10.1179/mnt.2001.110.1.27.

[3] Mortazavi, A., Osserbay, B. (2021) .The Consolidated Mathews Stability Graph for Open Stopee Design. Geotech. Geol. Eng, 40, 2409–2424. Doi: https://doi.org/10.1007/s10706-021-02034-0.

[4] Suorineni, F., Kaiser, P., & Tannant, D. (2000). Unifying application of the stability graph for open stopee design. *CIM Bulletin*.

[5] Mawdesley, C.A. (2004). Using logistic regression to investigate and improve an empirical design method. *Int. J. Rock Mech. Min. Sci*, *41*, 756–761. Doi:https://doi.org/10.1016/j.ijrmms.2004.03.131.

[6] Potvin, Y. (1988). Empirical open stopee design in Canada (Doctoral dissertation, University of British Columbia). Doi: https://dx.doi.org/10.14288/1.0081130.

[7] Potvin, Y., Hudyma, M.R., & Miller, H.D.S. (1989) Design guidelines for open stopee support. *CIM Bulletin*, 82, (926), 53–62.

[8] Potvin, Y., & Hudyma, M. (2000). Open stopee mining in Canada. Proceedings of the MassMin2000, Brisbane. Carlton: AusIMM, 661e74.

[9] Nickson, S.D. (1992) Cable support guidelines for underground hard rock mine operations. (Master's thesis, University of British Columbia). Doi: https://dx.doi.org/10.14288/1.0081080.

[10] Hadjigeorgiou, J., Leclair, J., Potvin, Y. (1995). An update of the Stability Graph Method for open stope design. 97th Annual General Meeting of C.I.M. Halifax, Nova Scotia.

[11] Trueman, R. Mikula, P. Mawdesley, C., & Harries, N., (2000). Experience in Australia with the application of the Mathew's method for open stope design. CIM-Bull. 2000 Jan; 93(1036):p 162-167.

[12] Stewart, S. V., & Forsyth, W. W. (1995). The Mathews method for open stopee design. CIM Bull, 45-53. Doi: 10.1016/0148-9062(96)85121-7.

[13] Mawdesley, C., Trueman, R., & Whiten, W. (2001). Extending the mathews stability graph for open stope design Trans. IMM (Section A). Volume 110, p A27-39.

Doi: https://doi.org/10.1179/mnt.2001.110.1.27.

[14] Suorineni, F.T. (2010). The stability graph after three decades in use: Experiences and the way forward. International Journal of Mining, Reclamation & Environment, 24, 307–339. Doi: https://doi.org/10.1080/17480930.2010.501957.

[15] Suorineni, F.T., & Madenova, Y. (2022). The qualitative stability graph for open stopee design- recent developments. Paper presented at the 56th U.S. Rock Mechanics/Geomechanics Symposium, Santa Fe, New Mexico, USA, June 2022. Doi: https://doi.org/10.56952/ARMA-2022-0017

[16] Milne, D. M., Pakalnis, R. C., & Lunder, P. J. (1996). Approach to the quantification of hanging-wall behaviour. Transactions of the Institution of Mining & Metallurgy. Section A: Mining Industry, 105, 69–74.

[17] Milne, D.M., Pakalnis, R.C., & Felderer, M. (1996). Surface geometry assessment for open stopee dsign, Proceedings of North America Rock Mechanics Symposium, Kingston. Doi: 10.22044/tuse.2023.12860.1475

[18] Milne, D.M. (1997). Underground Design and Deformation based on surface geometry. (PhD thesis, The University of British Columbia. Doi: 10.14288/1.0081050

[19] Milne, D.M., & Pakalnis, R. (1997) Theory behind empirical design techniques. Proceedings 12th colloque en controle de terrain, Assoc. Min, Québe.

[20] Germain, P., Hadjigeorgiou, J. (1998). Influence of stope geometry on mining performance, Proceedings of 100th Annual General Meeting, CIM, Vancouver, B.C., Canada.

[21] Milne, D., Pakalnis, R., Grant, D., & Sharma, J. (2004). Interpreting hanging wall deformation in mines. International Journal of Rock Mechanics & Mining Sciences, 41, 1139–1151. Doi: https://doi.org/10.1016/j.ijrmms.2004.05.004

[22] Henning, J.G., Mitri, H.S. (2006). Numerical modelling of ore dilution in blasthole. Doi: 10.1016/j.ijrmms.2006.11.002

[23] Andrews, P.G., Barsanti, B.J. (2008). Results of the Radius Factor Stability Assessment Method for Design and Pillar Extraction at the Conqueror Mine, St Ives Gold Mine. SHIRMS stopeing. Int. J. Rock Mech. Min. 44, 692–703.Doi: https://doi.org/10.36487/ACG_repo/808_06

[24] Milne, D., Snell, G. (2018). New failure prediction method for underground excavations. *CIM Journal*, Vol. 9, No. 1.

[24] Shaker, D., Milne, D.M., Eng, P., Hughes, P., & Schartner, N. (2018). Prediction of Hanging Wall Instability Using the Strain Effective Radius Factor Method, 52nd U.S. Rock Mechanics/Geomechanics Symposium, Seattle, Washington.

[26] Comparing Hydraulic Radius (HR) and Effective Radius Factor (ERF) Frans Basson (Basrock.net)

[27] Mohammadi, H., Fatehi Marji, M., Jalali, S.E., & Dabbagh, A. (2023). Analytical and comparative evaluation of empirical methods for stability studies on open stopeing with emphasis on stope geometry consideration. *Tunnelling and underground spacec engineering, Shahrood university of technology*, Vol.11, No 2, 199-216. Doi: 10.22044/tuse.2023.12860.1475

[28] Laubscher, D. H. (2000). A practical manual on block caving. Julius Kruttschnitt Mineral Research Centre, Brisbane.

[29] Hustrulid, W. A., Bullock, R. L., & Bullock, R. C. (2001). Underground Mining Methods: Engineering Fundamentals and International Case Studies. SME.

[30] Sakurai, S. (1983). Back analysis of measured displacements of tunnels. *Rock Mechanics and Rock Engineering*, 16(3), 173–180. https://doi.org/10.1007/BF01030209.

[31] Aydan, Ö., Akagi, T., & Kawamoto, T. (1993). The squeezing potential of rocks around tunnels: Theory and prediction techniques. *Rock Mechanics and Rock Engineering*, 26(3), 137–163. https://doi.org/10.1007/BF01020287.

[32] Chern, J. C., Juang, J. C., Chou, C. K., Lo, C. M., & Cheng, Y. M. (1998). Monitoring and back analysis of a collapsed tunnel in Taiwan. *Tunneling and Underground Space Technology*, 13(2), 143–150. https://doi.org/10.1016/S0886-7798 (98)00046-2.

[33] Hook, J. J. (2001). Geotechnical and structural performance of deep excavations in soft ground (Doctoral dissertation, University of Cambridge).

[34] Singh, B., Goel, R. K., & Jethwa, J. L. (2007). Tunneling through weak rocks: Concepts and practical applications. Elsevier.

[35] Hartman, Howard L. (1992) SME Mining Engineering Handbook, Published by the Society for Mining, Metallurgy and Exploration, Inc. Littleton, Colorado, USA, pp. 1717.